2016-08-01

The intact Kunitz domain protects the amyloid precursor protein from being processed by matriptase-2

Beckmann, A-M

10.1515/hsz-2015-0263
Biological Chemistry
De Gruyter

Biological Chemistry ‘Just Accepted’ Papers

Biological Chemistry ‘Just Accepted’ Papers are papers published online, in advance of appearing in the print journal. They have been peer-reviewed, accepted and are online published in manuscript form, but have not been copy edited, typeset, or proofread. Copy editing may lead to small differences between the Just Accepted version and the final version. There may also be differences in the quality of the graphics. When papers do appear in print, they will be removed from this feature and grouped with other papers in an issue.

Biol Chem ‘Just Accepted’ Papers are citable; the online publication date is indicated on the Table of Contents page, and the article’s Digital Object Identifier (DOI), a unique identifier for intellectual property in the digital environment (e.g., 10.1515/hsz-2011-xxxx), is shown at the top margin of the title page. Once an article is published as **Biol Chem ‘Just Accepted’ Paper** (and before it is published in its final form), it should be cited in other articles by indicating author list, title and DOI.

After a paper is published in **Biol Chem ‘Just Accepted’ Paper** form, it proceeds through the normal production process, which includes copy editing, typesetting and proofreading. The edited paper is then published in its final form in a regular print and online issue of **Biol Chem.** At this time, the **Biol Chem ‘Just Accepted’ Paper** version is replaced on the journal Web site by the final version of the paper with the same DOI as the **Biol Chem ‘Just Accepted’ Paper version.**

Disclaimer

Biol Chem ‘Just Accepted’ Papers have undergone the complete peer-review process. However, none of the additional editorial preparation, which includes copy editing, typesetting and proofreading, has been performed. Therefore, there may be errors in articles published as **Biol Chem ‘Just Accepted’ Papers** that will be corrected in the final print and online version of the Journal. Any use of these articles is subject to the explicit understanding that the papers have not yet gone through the full quality control process prior to advanced publication.

Biological Chemistry **'Just Accepted' paper**
ISSN (online) 1437-4315
DOI: 10.1515/hsz-2015-0263

Research Article

The intact Kunitz domain protects the amyloid precursor protein from being processed by matriptase-2

Anna-Madeleine Beckmann[1], Konstantin Glebov[2], Jochen Walter[2], Olaf Merkel[2], Martin Mangold[1], Frederike Schmidt[3], Christoph Becker-Pauly[3], Michael Gütschow[1] and Marit Stirnberg[1,]*

[1]Pharmaceutical Institute, University of Bonn, An der Immenburg 4, D-53121 Bonn, Germany

[2]Department of Neurology, University of Bonn, Sigmund-Freud-Str. 25, D-53127 Bonn, Germany

[3]Institute of Biochemistry, Unit for Degradomics of the Protease Web, Christian Albrechts University, Rudolf-Höber-Str. 1, D-24118 Kiel, Germany

*Corresponding author

e-mail: marit.stirnberg@uni-bonn.de

Abstract

Proteolytic processing of the amyloid precursor protein (APP) leads to amyloid-β (Aβ) peptides. So far, the mechanism of APP processing is insufficiently characterized at the molecular level. Whereas the knowledge of Aβ generation by several proteases has been expanded, the contribution of the Kunitz-type protease inhibitor domain (KPI) present in two major APP isoforms to the complex proteolytic processing of APP is poorly understood. In this study, we have identified KPI-containing APP as a very potent, slow-binding inhibitor for the membrane-bound proteolytic regulator of iron homeostasis matriptase-2 by forming stable complexes with its target protease in HEK cells. Inhibition and complex formation depend on the intact KPI domain. By inhibiting matriptase-2, KPI-containing APP is protected from matriptase-2-mediated proteolysis within the Aβ region, thus preventing the generation of N-terminally truncated Aβ.

Keywords: amyloid β; enzyme kinetics; iron homeostasis; Kunitz inhibitor; type II transmembrane serine protease.

Introduction

Matriptase-2 (MT2; the corresponding gene name is *TMPRSS6*) was shown to be a critical proteolytic regulator controlling iron metabolism. This was evidenced by patients with mutations in *TMPRSS6* suffering from iron-refractory iron deficiency anaemia (IRIDA) (Finberg *et al.*, 2008) and by murine models with an anaemic and iron deficient phenotype (Du *et al.*, 2008; Finberg *et al.*, 2010; Folgueras *et al.*, 2008). It has been demonstrated that matriptase-2 downregulates hepcidin expression *via* BMP/SMAD signaling, probably by cleaving the BMP co-receptor hemojuvelin which was shown *in vitro* (Maxson *et al.*, 2010; Silvestri *et al.*, 2008). Matriptase-2-mediated hemojuvelin cleavage *in vivo* is under investigation (Krijt *et al.*, 2011).

Matriptase-2 belongs to the type II transmembrane serine proteases (TTSPs) within the superfamily of trypsin-like serine proteases which was discovered in 2002 (Hooper *et al.*, 2001; Velasco *et al.*, 2002). This protease comprises a short N-terminal cytoplasmic tail and a large extracellular domain, the latter is divided into the stem region with the SEA domain, two CUB domains and three LDL receptor class A domains, and the protease domain. Matriptase-2 shares high similarities to the close homologue matriptase, involved in epidermal differentiation, which is tightly regulated by its cognate Kunitz-type inhibitor hepatocyte growth factor activator inhibitor-1 (HAI-1) (Bugge *et al.*, 2007; Lin *et al.*, 1999; Miller and List, 2013). Recently, we have found matriptase-2 to be inhibited by Kunitz-type inhibitor hepatocyte growth factor activator inhibitor-2 (HAI-2) in a cell system co-expressing both proteins (Maurer *et al.*, 2013).

In this study, the amyloid precursor protein (APP) was identified as another candidate inhibitor for matriptase-2 in cell-free and cell-based assays. APP is an ubiquitously expressed type I transmembrane protein discovered in 1987 (Goldgaber *et al.*, 1987) with a still unknown physiological function. It is one of the most studied proteins since it has been implicated in the pathogenesis of Alzheimer's disease (AD) (LaFerla and Oddo, 2005; Zheng and Koo, 2011). One of the pathologic hallmarks of AD is the accumulation of insoluble, extracellular amyloid plaques in the brain which are mainly composed of Aβ peptides derived from APP processing (Selkoe 1991). In the amyloidogenic pathway, cleavage of APP by β-site APP-cleavage enzyme 1 (BACE1) generates a membrane-bound C-terminal fragment (CTFβ) which is subsequently cleaved by the γ-secretase complex generating neurotoxic Aβ

peptides (Sastre *et al.*, 2001; Vassar *et al.*, 1999). The generation of Aβ peptides is prevented by processing of APP *via* the non-amyloidogenic pathway in which the α-secretase cleaves within the Aβ domain producing an extracellular soluble form of APP (sAPPα) with neuroprotective properties (Sisodia 1992).

Three major isoforms APP695, APP751 and APP770 are known. The latter two contain a Kunitz-type protease inhibitor domain (KPI) of 51 amino acids located in the middle of the ectodomain and are widely expressed in non-neuronal cells whereas APP695, lacking the KPI domain, is the predominant isoform found in brain. The amino acid sequence of APP770 is shown in Figure 1A. The KPI domain of APP was shown to inhibit serine proteases *in vitro* such as trypsin and chymotrypsin (Bhasin *et al.*, 1991; Shimokawa *et al.*, 1993; Van Nostrand *et al.*, 1989; Van Nostrand *et al.*, 1990), and factors XIa and IXa (Schmaier *et al.*, 1995).

In this study, the inhibitory potential of KPI-containing APP towards matriptase-2 was determined by kinetic analysis. Additionally, the impact of KPI-mediated matriptase-2 inhibition on APP processing was characterized. Our results indicate that the KPI domain protects APP from being degraded by matriptase-2. Uninhibited matriptase-2 processes APP to generate N-terminally truncated Aβ(6-40) in cell culture experiments.

Results

APP inhibits matriptase-2 in a cell-based system

Recently, we have found matriptase-2 to be inhibited by the Kunitz-type inhibitor HAI-2 in a cell system co-expressing both proteins (Maurer *et al.*, 2013). In order to validate whether KPI-containing APP inhibits matriptase-2 we co-expressed APP770 in HEK cells stably transfected with matriptase-2. For this, a vector encoding matriptase-2 C-terminally fused to a Myc- and His-tag and a vector encoding isoform APP770 containing KPI N-terminally fused to a Strep-tag were used (Figure 1). Matriptase-2 activity was measured in membrane fractions as well as concentrated conditioned media derived from matriptase-2-transfected HEK cells with the peptide substrate Boc-QAR-*para*-nitroanilide (Figure 2A) as reported previously (Stirnberg *et al.*, 2010). In contrast, HEK-mock and APP770 expressing cells did not display any measurable activity. Interestingly, matriptase-2 activity was drastically diminished after co-expressing APP770 and matriptase-2 indicating that APP770 bears the potential to inhibit matriptase-2 proteolytic activity in a cell-based system.

Inhibition of matriptase-2 by APP770 was also demonstrated by determining the activity of cell surface-associated matriptase-2 on intact HEK-MT2-Myc-His cells in the presence of recombinant soluble APP770 (sAPP770). For this, sAPP770 was purified from conditioned media of transfected HEK cells (Figure S1A). While HEK-mock cells did not show any activity, the used fluorogenic peptide substrate Boc-QAR-7-amido-4-methylcoumarin (AMC) was cleaved by HEK-MT2-Myc-His cells with a more moderate activity in the presence of 30 nM sAPP770 (Figure 2B). By applying these two different methods for assaying matriptase-2 activity, the Kunitz-type inhibitor APP770 has been newly identified as an inhibitor of matriptase-2.

APP770 acts as a potent, slow-binding inhibitor for matriptase-2

In a next step, we characterized the inhibitory potency of APP770 against matriptase-2. For this, purified recombinant sAPP770 was incubated with conditioned media derived from matriptase-2-expressing HEK cells in the presence of the fluorogenic substrate Boc-QAR-AMC. Efficient shedding of active matriptase-2 allows the usage of concentrated media for enzyme kinetics (Dosa *et al.*, 2012; Maurer *et al.*, 2012; Sisay *et al.*, 2010; Stirnberg *et al.*, 2010). The progress curves in the presence of different inhibitor concentrations were non-linear in the pre-equilibrium phase and approached linearity to achieve the binding equilibrium (Figure 2C) showing time dependent inhibition in the course of the assay. Hence, sAPP770 acts as a slow-binding inhibitor and the progress curves were analyzed by non-linear regression using the slow-binding equation. The replot of k_{obs} values versus inhibitor concentrations [sAPP770] was linear (Figure 2D; inset) and the on ($k_{on} = 5.0\times10^{-4}$ s^{-1} nM^{-1}) and off ($k_{off} = 8.0\times10^{-4}$ s^{-1}) rate constants for inhibitor association/dissociation were obtained. The inhibition constant K_i of 0.66 ± 0.02 nM was calculated from the steady state rates of the progress curves, which were plotted versus the inhibitor concentration (Figure 2D) to obtain the IC_{50} value, from which the K_i value was calculated. In summary, the kinetic analyses confirmed a reversible, slow-binding mode of interaction indicating that sAPP770 binds to the active site of matriptase-2 in a substrate-like manner as proposed for Kunitz-type inhibitors (Eigenbrot *et al.*, 2010; Farady and Craik, 2010). The same analysis was performed with the purified isoform sAPP751 also containing KPI. This isoform exhibited a K_i value in exactly the same low nanomolecular range as sAPP770 (Figure S2A and B) whereas sAPP695 and sAPP770$^{\Delta KPI}$, both containing no KPI domain, did not inhibit matriptase-2 (Figure S2C and D). In conclusion, the two KPI-containing sAPP770 and sAPP751 have equal inhibitory

potencies towards matriptase-2 while KPI-lacking sAPP695 and sAPP770$^{\Delta KPI}$ were ineffective.

Matriptase-2 forms complexes with APP770

As Kunitz-type inhibitors are known to form stable, SDS-resistant complexes with their target proteases, formation of complexes was analyzed by western blotting in HEK cells transfected with matriptase-2 and APP770. Matriptase-2 was detected with a molecular weight of ca. 120 kDa in membrane fractions derived from HEK cells expressing matriptase-2 by the use of the c-Myc antibody after separating the proteins under reducing and non-reducing conditions (Figure 3A and B; left panels; lanes 4 and 5). Matriptase-2 undergoes a complex auto-processing mechanism resulting in cell surface release of a two-chain form (Jiang *et al.*, 2014; Stirnberg *et al.*, 2010). After its synthesis as a membrane-bound, inactive one-chain zymogen of ca. 120 kDa, matriptase-2 is shed into the surrounding medium as an activated two-chain form of about 55 kDa comprising the protease domain of ca. 30 kDa tethered *via* a conserved disulfide bond to a portion of the stem region (Stirnberg *et al.*, 2010). For this reason, the 30 kDa protease domain was detectable in the conditioned media of matriptase-2-expressing cells after separating the samples under reducing conditions (Figure 3A; right panel; lanes 8 and 9) whereas under non-reducing conditions the disulfide-linked two-chain form of matriptase-2 of ca. 55 kDa was visible (Figure 3B; right panel; lanes 8 and 9). Interestingly, after co-expressing APP770, two additional matriptase-2-specific signals occurred in the conditioned media of ca. 130 and 170 kDa (Figure 3B; right panel; lane 9, asterisks) indicating that matriptase-2 is bound to interaction partners that are presumably distinct shed forms of APP770.

APP-specific signals were detected by the use of Strep-Tactin AP conjugate in membrane fractions and in conditioned media of APP770-transfected cells of ca. 120 kDa (Figure 3C and D; left and right panels; lanes 3, 5, 7 and 9). The presence of soluble APP in conditioned media indicated cell surface release of APP770 in our cell system generated by α-secretase (sAPPα). Notably, after separating proteins of conditioned media under non-reducing conditions, a further signal of ca. 170 kDa was visible after co-expressing matriptase-2 (Figure 3D; right panel; lane 9, asterisk) again demonstrating that APP770 is bound to matriptase-2. Beside this, an additional band of ca. 95 kDa suggested that matriptase-2 is presumably able to cleave APP770. These results show that matriptase-2 and APP770 interact to form stable, SDS-resistant complexes. APP770 was confirmed as an interaction partner of

matriptase-2 by purification of c-Myc-tagged matriptase-2 *via* the affinity to Strep-tagged APP770 bound to immobilized Strep-Tactin (Figure 4).

Matriptase-2 inhibition by APP770 depends on intact KPI

We next analyzed whether the inhibitory potential of APP770 against matriptase-2 and/or formation of the matriptase-2/APP complex depends on KPI of APP770. For this purpose, different mutated variants of APP770 were co-expressed in matriptase-2-transfected cells in which the whole KPI (ΔKPI) was deleted or a specific arginine residue was mutated. The canonical active site of Kunitz-domain containing proteins was identified as Arg^{260} in case of Kunitz domain I of HAI-1 (Lin *et al.*, 2008) that assigned the inhibitory specificity against trypsin-like serine proteases which are characterized to show a clear preference for arginine residues in P1 position. Therefore, the corresponding Arg^{301} in KPI of APP770 was mutated to Glu in R301E (Figure 1A). As expected, APP770 with mutated ΔKPI and R301E failed to inhibit matriptase-2 to a similar extent as wild type APP770 (Figure 5A). This is in line with the absence of an inhibitory potency of purified KPI-lacking sAPP695 or $sAPP770^{\Delta KPI}$ towards matriptase-2 (Figure S2C and D). In sum, these results show that KPI and specifically the amino acid Arg^{301} are critical in determining the inhibitory potential of APP against matriptase-2.

Formation of APP/matriptase-2 complexes depends on intact KPI

Additionally, we analyzed whether the lack of inhibitory capacity of the APP770 mutants correlates with the inability to form stable complexes with matriptase-2. For this reason, protein samples were separated under non-reducing conditions prior to Western blotting to maintain protein/protein interactions. In conditioned media, the soluble wild type and mutated APP770 fragments of ca. 120 kDa appeared (Figure 5B; lanes 3, 5 and 7) indicating that the mutated APP770 variants were released from the cell surface. Again, co-expression of wild type APP770 with matriptase-2 revealed the 170 kDa-complex and the cleaved 95 kDa-fragment beside the 120 kDa-fragment (Figure 5B; lane 4; 170 kDa-complex marked with an asterisk). Notably, the complex at 170 kDa was absent in the generated APP770 mutants (Figure 5B; lanes 6 and 8). Moreover, co-expression of matriptase-2 with mutated APP770 completely abolished the 120 kDa-fragment and increased the signal of the cleaved 95 kDa-fragment (Figure 5B; lanes 6 and 8). Expression of wild type and mutated APP770 at ca. 120 kDa was confirmed in membrane fractions (Figure 5C; lanes 3 to 8).

Using a c-Myc antibody, matriptase-2 was visible at 55 kDa in conditioned media of single transfected cells (Figure 5D; lane 2). In co-transfected cells matriptase-2-specific signals occurred at ca. 55, 130 and 170 kDa (Figure 5D; lane 4; 170 and 130 kDa-complexes marked with asterisks). After co-expressing the mutated APP770 variants, complexes at ca. 130 and 170 kDa were missing (Figure 5D; lanes 6 and 8) reflecting the results obtained by APP detection. In membrane fractions, matriptase-2 was again visible at ca. 120 kDa (Figure 5E; lanes 2, 4, 6 and 8). These results indicate that the mutated variants of APP770 being affected in their KPI domain obviously failed to form complexes with matriptase-2 according to their impaired inhibitory potential against matriptase-2.

Matriptase-2 generates truncated versions of APP

Expression of matriptase-2 resulted in the secretion of an additional fragment of APP770 into the conditioned media that migrates below (~95 kDa) the secreted sAPPα fragment generated by α-secretase (~120 kDa) (Figure 3D; right panel; lane 9 and Figure 5B; lane 4). Thus, wild type APP770 did not serve merely as an inhibitor but also as a substrate of matriptase-2. Since the Strep-tag fused to the N-terminus was used for detection of APP (Figure 1B), matriptase-2 is able to generate C-terminally truncated versions of soluble APP770 in this cell system. Furthermore, after diminishing the inhibitory potential of APP770 by expressing the mutated versions affected in KPI, the apparent molecular mass of secreted APP770 shifted from 120 kDa to 95 kDa (Figure 5B; lanes 6 and 8). These results show that matriptase-2 cleaves APP efficiently in case it is not inhibited by the APP KPI domain. In summary, the KPI domain is likely to protect APP from being degraded by matriptase-2 in our cell system.

In order to analyze if matriptase-2 is involved in the generation of Aβ peptides, two quenched fluorogenic peptide substrates, M2460 and M2465, derived from amino acids 667 to 676 of human APP770 wild type (M2460) and human APP770 Swedish mutant (M2465) representing the β-secretase cleavage site (Figure 6A) were tested for their susceptibility to be cleaved by matriptase-2. Both substrates were efficiently cleaved by matriptase-2 in conditioned media of HEK-MT2-Myc-His cells (Figure 6B). As mentioned above matriptase-2 has a clear preference to cleave after positively charged amino acids. Thus, cleavage of M2460 can potentially occur after Lys^{670} and/or Arg^{676}. However, cleavage of the substrate M2465, in which Lys^{670} is mutated to Asn, clearly indicated that Arg^{676} in P1 position was targeted by matriptase-2.

Arg^{676} lies within the Aβ peptide region close to the N-terminus at amino acid position 5 (Figure 1A). Therefore, we analyzed the generation of secreted Aβ peptides in dependence on matriptase-2 expression using wild type APP770, $APP770^{\Delta KPI}$ and double mutant $APP770^{\Delta KPI/R676E}$. The Aβ peptides were immunoprecipitated from conditioned media of transfected HEK cells with antibody 4G8 recognizing an epitope within amino acids 18-22 of Aβ (Figure 1A) prior to immunoblotting with this antibody. As shown in Figure 7A (lower panel, lanes 1, 3 and 5) Aβ was generated after expression of APP. Aβ was also produced in the presence of matriptase-2 (Figure 7A, lower panel, lane 2). However, after co-expression of matriptase-2 and $APP770^{\Delta KPI}$ a shift to a smaller Aβ peptide variant was observed (Figure 7A, lower panel, lane 4) indicating that matriptase-2 cleaves APP within the Aβ domain. In accord with this result, a larger CTF was additionally present in membrane fractions of these cells (Figure 7A, middle panel, lane 4). Assuming that the shorter version of the CTFs was generated by the α-secretase cleavage (CTFα) the larger matriptase-2 generated version (CTF_{MT2}) occurred by cleavage at Arg^{676}. This is further supported by the absence of the higher molecular weight CTF_{MT2} in $APP770^{\Delta KPI/R676E}$ and matriptase-2-expressing cells (Figure 7A, middle panel, lane 6). However, a shift to a smaller Aβ peptide was still observable in this sample although the putative matriptase-2 cleavage site Arg^{676} was mutated indicating that matriptase-2 can additionally cleave Aβ at another position.

Because antibody 4G8 not only detects Aβ, but also the p3 peptide that is generated by the α-secretory processing and subsequent cleavage of the CTF by γ-secretase we have also used the N-terminal neoepitope-specific antibody 82E1 recognizing amino acids 1-5 of the Aβ peptide. Again, detection of Aβ was possible after transfection of APP (Figure 7B, lower panel, lanes 3 and 5) verifying the generation of Aβ in these cells. Interestingly, co-expression of $APP770^{\Delta KPI}$ and matriptase-2 completely abolished the Aβ signal detectable by antibody 82E1 (Figure 7B, lower panel, lane 6) although Aβ was present in this sample as shown by using antibody 4G8 (Figure 7A, lower panel, lane 4), thereby confirming that matriptase-2 cleaves within the N-terminal region of Aβ. The absence of the signal after co-expressing matriptase-2 and the mutated variant $APP770^{\Delta KPI/R676E}$ (Figure 7B, lower panel, lane 8) may result from the inability to detect the mutated neoepitope. Accordingly, the Aβ signal in lane 7 could be derived from endogenously expressed APP which was also detectable as shown in lane 1 (Figure 7B, lower panel).

Cleavage at Arg^{676} by matriptase-2 was further indicated by the absence of sAPPα in conditioned media of cells co-expressing matriptase-2 and the mutated variant $APP770^{\Delta KPI}$

using antibody 6E10 (Figure 7B, upper panel, lane 6). This antibody recognizes an epitope within amino acids 3-8 of the Aβ region. We postulated that after cleavage at Arg^{676}, $sAPP_{MT2}$ was generated which escaped detection by antibody 6E10. The absence of the signal after co-expressing matriptase-2 and the mutated variant $APP770^{\Delta KPI/R676E}$ (Figure 7B, upper panel, lane 8) may again result from the inability to detect the mutated epitope and the presence of the signal in lane 7 may be derived from Aβ generated from endogenously expressed wild type APP.

To verify Aβ processing by matriptase-2 at position Arg^{676} in our cell-based system, mass spectrometric analyses were performed with samples derived from conditioned media of HEK-mock and HEK-MT2-Myc-His cells transfected with the mutated variant $APP770^{\Delta KPI}$ after immunoprecipitation with antibody 4G8. These samples were already analyzed by western blotting resulting in a shift to a smaller Aβ peptide in the presence of matriptase-2 (Figure 7A, lower panel, lanes 3 and 4). MALDI-TOF analyses revealed the presence of Aβ(1-40) derived from cells expressing $APP770^{\Delta KPI}$ (Figure 8). Concurrently with the observed shift to a smaller Aβ peptide variant by western blottng, Aβ (6-40) was detectable by MALDI-TOF analyses instead of Aβ(1-40) after simultaneous expression of $APP770^{\Delta KPI}$ and matriptase-2 undoubtedly confirming the cleavage site at position Arg^{676} targeted by matriptase-2. Additionally, Aβ(5-40) disappeared after co-expression of matriptase-2, possibly due to degradation to Aβ(6-40) by matriptase-2 (Figure 8). In HEK-mock cells Aβ(1-37/38) was detected (Figure 8, upper spectrum), presumably degraded to Aβ(6-37/38) in the presence of matriptase-2 (Figure S3).

In a further experiment synthetic Aβ(1-42) was incubated with recombinant matriptase-2. As a control, synthetic Aβ(1-42) was incubated alone. While MALDI-TOF measurements revealed the presence of full length Aβ(1-42) in both samples (Figure S4) the application of LC-MS analysis identified Aβ peptides cleaved by matriptase-2. Indeed, Aβ(6-17) and Aβ(6-28) were found (Table 1) indicating that matriptase-2 cleaved at site Arg^{676}.

Discussion

Whilst the proteases involved in APP processing have been studied intensively during the past years, the mechanism of controlling the activity of processing proteases due to the action of APP itself is largely unknown. APP exists in three major isoforms with unknown functions

from which two of them comprise a KPI domain bearing the potential to inhibit several serine proteases (Bhasin *et al.*, 1991; Schmaier *et al.*, 1995; Shimokawa *et al.*, 1993; Van Nostrand *et al.*, 1989, 1990). In our study, we have identified KPI-containing APP770 as a very potent inhibitor of the serine protease matriptase-2 by forming stable complexes depending on one critical arginine residue in APP, Arg^{301} in a transfected cell system. Due to its high inhibitory potential, KPI-containing APP770 is protected from being degraded by the overexpressed matriptase-2. Remarkably, APP770 did not inhibit the intrinsic activity of matriptase-2 zymogen since the two processing events catalyzed by matriptase-2 itself, activation and shedding (Stirnberg *et al.*, 2010), were detectable by the presence of a 30 kDa-fragment in conditioned media of matriptase-2 and APP770 expressing HEK cells (Figure 3A, lane 9). This could be due to a lower affinity of KPI-containing APP770 for the inactive zymogen than for the activated protease.

Interestingly, in our cell system APP770 serves as an inhibitor and likewise as a substrate depending on the presence of the KPI domain. The deletion of the KPI domain changed the role of APP from being an inhibitor to being a substrate for matriptase-2. Matriptase-2 hydrolyzes peptide bonds after basic amino acids with a clear preference for arginine over lysine in P1 position (Velasco *et al.*, 2002). Accordingly, we could identify Arg^{676} (corresponding to Aβ5) within the N-terminal region of the Aβ domain which is cleaved by matriptase-2 by MALDI-TOF analyses after co-expressing $APP770^{\Delta KPI}$ and matriptase-2. Other sites, probably Lys^{687} (corresponding to Aβ16) which is the α-secretase cleavage site and Lys^{699} (corresponding to Aβ28), may also be targeted by matriptase-2 as shown by LC-MS analysis of a synthetic Aβ peptide after incubation with recombinant matriptase-2 (Table 1) and by western blot analysis of Aβ after co-expressing $APP770^{\Delta KPI/R676E}$ and matriptase-2 (Figure 7A, lower panel, lane 6). The shift to a smaller Aβ peptide variant in this sample indicated the presence of at least one additional cleavage site beside Arg^{676} that is presumably Lys^{699}. Cleavage at this site would generate Aβ(1-28) with a similar molecular weight like Aβ(6-40).

Additionally, matriptase-2 seems to target APP770 beside the Aβ domain. After co-expressing matriptase-2 and KPI-containing APP770, a smaller complex of 130 kDa appeared beside the 170 kDa-complex as observed by the use of the c-Myc-antibody (Figure 3B, lane 9). Because this smaller 130 kDa-complex could not be seen after detection of Strep-tagged APP770 (Figure 3D, lane 9), APP770 is presumably N-terminally truncated resulting in the loss of the Strep-tag.

A proposed model of matriptase-2 mediated processing of APP770 is shown in Figure 9. In our cell system, processing of KPI-containing APP770 can occur predominantly by α-secretase described as the non-amyloidogenic pathway producing sAPPα detectable in conditioned media and CTFα detectable in membrane fractions. The occurrence of these APP fragments, sAPPα and CTFα, is independent on matriptase-2 co-expression. Smaller amounts of APP770 can be processed by the amyloidogenic pathway since Aβ, presumably Aβ(1-40), was detectable in conditioned media. If APP is expressed without the KPI domain matriptase-2 becomes active and catalyzes the cleavage after position Arg^{676}. The cleavage may occur in full length APP generating $sAPP_{MT2}$ and CTF_{MT2}. The latter can be converted to Aβ(6-40) by the γ-secretase. Matriptase-2 cleavage may also occur in CTFβ liberating CTF_{MT2}, in Aβ(1-40) liberating Aβ(6-40) and in sAPPα liberating $sAPP_{MT2}$. As a consequence, in $APP770^{\Delta KPI}$ and matriptase-2 co-expressing cells, $sAPP_{MT2}$, CTFα, CTF_{MT2} and Aβ(6-40) were present in detectable levels.

Taken together, we have demonstrated for the first time that the KPI domain determines the susceptibility of APP to proteolytic cleavage by the serine protease matriptase-2 in HEK cells. The proteolysis of APP by matriptase-2 generating, amongst others, N-terminally truncated Aβ peptides solely depends on the presence of KPI. Future experiments are necessary to analyze the biological relevance of matriptase-2-mediated APP processing. Additionally, it has to be elucidated whether KPI-containing APP is involved in iron homeostasis by regulating matriptase-2 activity. A link between APP and iron homeostasis was already suggested by describing an iron-responsive element in the 5`-untranslated region of the APP transcript (Rogers *et al.*, 2002) and by reporting an interaction of APP and the iron exporter ferroportin (Wong *et al.*, 2014). Recently, matriptase-2 was identified as a cell surface activator of metalloprotease meprin β thereby enhancing APP shedding (Jäckle *et al.*, 2015).

Materials and methods

Cell lines and culture conditions

Human embryonic kidney (HEK) 293 cells (Graham *et al.*, 1977) were cultured in Dulbecco's modified Eagle's medium. Huh-7 cells were cultured in RPMI medium. Cells were cultured under a humidified atmosphere of 5% CO_2 at 37°C. Both media were supplemented with penicillin (100 U/ml), streptomycin (100 µg/ml), and fetal bovine serum (FBS) (10%).

Additionally, Huh-7 cells were cultured in medium supplemented with glutamine (2 mM) and non-essential amino acids (0.1 mM; all substances and media from Life Technologies, Karlsruhe, Germany).

Cloning

The construction of the expression plasmids pcDNA4 and pcDNA4-MT2-Myc-His, and the generation of stably transfected HEK-MT2-Myc-His cells were described previously (Stirnberg *et al.*, 2010).

For the generation of all other plasmids total mRNA was isolated from Huh-7 cells with TRIZOL-Reagent (Life Technologies) and transcribed into cDNA using Omniscript RT kit (Qiagen, Hilden, Germany) and Oligo(dT) primer (Life Technologies) according to the instruction manuals. For the expression of APP770 (Leu^{18}-Asn^{770}) with a Strep-tag at the N-terminus, the whole *APP* open reading frame was amplified using primers 5'-GCT CCC **GGT CTC** TGC GCC CTG GAG GTA CCC ACT GAT GG-3' and 5'-GCT CCC **GGT CTC** TGG CCC TAG TTC TGC ATC TGC TCA AAG-3' (BsaI recognition sites in bold, *APP* cDNA underlined) digested with BsaI and ligated into the BsaI-digested expressing vector pEXPR-IBA44 (IBA, Göttingen, Germany) to generate pEXPR-Strep-APP770.

This vector was used to generate pEXPR-Strep-$APP770^{\Delta KPI}$ encoding APP770 without the KPI domain by splicing by overlapping extension PCR with primers 5'-GCT CCC **GGT CTC** TGC GCC CTG GAG GTA CCC ACT GAT GG-3' and 5'-CTT TGG GAC ATG GCG CTG CCC ACC TCT CGA ACC ACC TCT T-3' for the amplification of the *APP*-encoding cDNA upstream of the KPI-encoding sequence, and 5'-AAG AGG TGG TTC GAG AGG TGG GCA GCG CCA TGT CCC AAA G-3' and 5'-GCT CCC **GGT CTC** TGG CCC TAG TTC TGC ATC TGC TCA AAG-3' for the amplification of the cDNA downstream of the KPI-encoding sequence. The vector pEXPR-Strep-APP770 was also subjected to site directed mutagenesis with GeneArt Site-Directed Mutagenesis System (Life Technologies) according to the instruction manual using primers 5'-CGA GAC GGG GCC GTG CGA AGC AAT GAT CTC-3' and 5'-GCA CGG CCC CGT CTC GGC TTG TTC AGA G-3' to generate pEXPR-Strep-$APP770^{R301E}$. The vector pEXPR-Strep-$APP770^{\Delta KPI}$ was subjected to site directed mutagenesis using primers 5'-GGA TGC AGA ATT CGA ACA TGA CTC AGG ATA TG-3' and 5`-CAT ATC CTG AGT CAT GTT CGA ATT CTG CAT CC-3' to generate pEXPR-Strep-$APP770^{\Delta KPI/R676E}$.

Matriptase-2 activity assay of concentrated media and membrane fractions

Proteolytic activity measurements were performed with 5 µg total protein from concentrated media or 20 µg total protein of membrane fractions from HEK-mock or HEK-MT2-Myc-His cells either alone or transiently transfected with pEXPR-Strep-APP770, pEXPR-Strep-APP770$^{\Delta KPI}$ or pEXPR-Strep-APP770^{R301E} using 200 µM Boc-QAR-*para*-nitroanilide (Bachem, Bubendorf, Switzerland) as described previously (Stirnberg *et al.*, 2010).

Purification of sAPP770

HEK cells were grown in 175 cm^2-flasks. After transfection with 84 µg pEXPR-Strep-APP770, cells were cultured for two days with Opti-MEM. sAPP770 was isolated from the concentrated conditioned medium by affinity chromatography using the Strep-Tactin Sepharose column (IBA) following the manufacturer`s instructions. Purity of isolated sAPP770 was confirmed by SDS-PAGE (Figure S1) and concentration was determined by Bradford assay (Roti-Nanoquant; Carl Roth, Karlsruhe, Germany).

Matriptase-2 activity assay of intact cells

For measuring matriptase-2 proteolytic activity of intact cells, HEK-MT2-Myc-His cells or HEK-mock cells were grown on the surface of a 96-well plate. For this purpose, the cells were incubated in 200 µl of Dulbecco's modified Eagle's (DMEM)-medium (Gibco Life Technologies) to a confluence of approximately 70% under a humidified atmosphere of 5% CO_2 at 37°C. After removing DMEM, assay buffer (50 mM Tris-HCl, 150 mM NaCl, pH 8.0) and 30 nM of purified sAPP770 were added to each well. The reaction was started immediately by adding 0.8 µl of the fluorogenic peptide substrate Boc-QAR-AMC (10 mM stock solution). The final concentration of the substrate was 40 µM. The reaction was followed at 37°C for 50 min with an excitation wavelength of 340 nm and emission wavelength of 460 using the Fluostar Optima Plate Reader (BMG Labtech, Offenburg, Germany).

Kinetics of matriptase-2 inhibition

Inhibition assays of matriptase-2 in concentrated media of stably transfected HEK-MT2-Myc-His cells in the presence of different concentrations of purified APP were performed by monitoring the release of 7-amino-4-methylcoumarin from the fluorogenic substrate

Boc-QAR-AMC using Fluostar Optima Plate Reader (BMG Labtech). Reactions were monitored with an excitation wavelength of 340 nm and emission wavelength of 460 nm over 50 min at 37°C in a total volume of 200 µl assay buffer (50 mM Tris-HCl, 150 mM NaCl, pH 8.0) in the presence of 40 µM substrate and different APP concentrations (2 to 10 nM).

Progress curves of the reactions were analyzed by nonlinear regression using the slow-binding equation $[P] = v_s \times t + (v_i - v_s) \times (1 - \exp(-k_{obs} \times t))/k_{obs} + d$ to give v_s, v_i and k_{obs}, where [P] is the product concentration, v_s is the final steady-state rate, v_i is the initial rate, k_{obs} is the observed first-order rate constant for the approach to steady-state, and d is the offset. To obtain IC_{50} values for slow-binding inhibitors, v_s values from reactions in the presence of the inhibitor and v_s values obtained by linear regression of the uninhibited reaction in the time course between 2500 and 3000 s were used. This time course was chosen because of an observed curvature of the progress curves of the uninhibited reaction that did not result from substrate limitation. All kinetic measurements were carried out in duplicate with five different inhibitor concentrations. Mean v_s values were plotted versus the inhibitor concentrations [I], according to $v_s = v_0/(1+[I]/IC_{50})$ to obtain v_0 and IC_{50} values, where v_0 is the calculated rate of the reaction in the absence of the inhibitor. Standard errors (± SE) of these nonlinear regression analyses were determined. K_i values were calculated from equation $K_i = IC_{50}/(1+[S]/K_m)$ with a K_m value of 32.2 µM (Dosa *et al.*, 2012). The obtained k_{obs} values were replotted versus the inhibitor concentrations resulting in a linear correlation where k_{on}' was given by the slope and k_{off} by the ordinate-intercept. The k_{on} value was calculated using the equation $k_{on} = k_{on}'(1+[S]/K_m)$.

SDS-PAGE and immunoblotting

Stably transfected HEK-mock or HEK-MT2-Myc-His cells grown in 25 cm^2-flasks were transiently transfected with 12 µg pEXPR-Strep-APP770, pEXPR-Strep-APP770$^{\Delta KPI}$, pEXPR-Strep-APP770^{R301E} or pEXPR-Strep-APP770$^{\Delta KPI/R676E}$ by lipofection with Lipofectamine^{TM} 2000 (Life Technologies) in the presence of Opti-MEM (Life Technologies) according to the manufacturer's instructions. Fourty-eight hours after transfection, culture supernatants were concentrated and membrane fractions and lysates were isolated as described previously (Stirnberg *et al.*, 2010). An amount of 30 µg total protein from concentrated media, membranes or lysates were separated by SDS-PAGE (10% acrylamide) under non-reducing or reducing conditions and subjected to western blot analysis using monoclonal c-Myc antibody (clone 9E10; diluted 1:200) (Evan *et al.*, 1985) or monoclonal

anti-APP antibodies (4G8, diluted 1:1000; 6E10, diluted 1:100; both from Covance, Princeton, New Jersey, USA) and alkaline-phosphatase-conjugated secondary antibody (diluted 1:10000; Novagen, Merck, Darmstadt, Germany). Strep-tagged APP was also detected by using Strep-Tactin alkaline phosphatase conjugate (IBA). Detection was performed with NBT/BCIP (Nitro Tetrazolium Blue chloride/5-bromo-4-chloro-3-indolyl phosphate; Sigma-Aldrich, Saint Louis, USA). Transfer of proteins onto nitrocellulose membranes was validated by Ponceau S staining.

Co-purification of matriptase-2/APP complexes by affinity chromatography

For detection of complexes formed by matriptase-2/APP770, 400 µg total protein of conditioned media derived from HEK-MT2-Myc-His or HEK-mock cells transiently transfected with pEXPR-Strep-APP770, were subjected to affinity chromatography using the Strep-Tactin Sepharose column (IBA) according to the manufacturer's instructions. Elution fraction 3 was concentrated and subsequently analyzed by western blotting under reducing conditions using either the Strep-Tactin alkaline phosphatase conjugate for detection of APP770 or the c-Myc antibody for detection of matriptase-2.

Kinetics of APP cleavage by matriptase-2

To determine specific matriptase-2 cleavage sites within the APP amino acid sequence, two commercially available substrates covering the region from amino acids 667 to 676 harboring the β-secretase cleavage site were used (M2460, M2465; Bachem). Reactions were monitored with an excitation wavelength of 340 nm and emission wavelength of 460 nm over 20 min at 37°C in a total volume of 200 µl in the presence of 40 µM substrate and conditioned media from matriptase-2-expressing HEK cells or of conditioned media from HEK-mock cells. Assay buffer was 50 mM Tris-HCl, 150 mM NaCl, pH 8.0.

Detection of Aβ

Secreted Aβ was detected with monoclonal antibodies 4G8 (epitope 18-22; Covance) and 82E1 (neoepitope 1-5; IBL, Japan). While Aβ was directly detectable with antibody 82E1 (diluted 1:1000) after separating 30 µg of total protein from concentrated culture supernatants of transfected HEK cells under reducing conditions by NuPAGE (Novex, Life Technologies, Carlsbad, USA) using MES running buffer, detection of Aβ with antibody 4G8 required an immunoprecipitation prior the immunoblotting. For this, culture supernatants were removed

20 hours after transfection and supplemented with 10 µg of antibody 4G8. After incubation for 12 hours at 4°C, magnetic beads conjugated with Protein G (New England Biolabs, Frankfurt am Main, Germany) were applied according to the manufactory's instruction. Total protein of immunoprecipitation was separated by NuPAGE and subjected to Western blot analysis using antibody 4G8 (diluted 1:500). Horseradish peroxidase-conjugated secondary antibody was applied diluted 1:10 000. Chemiluminescence was detected using ECL advanced chemiluminescence kit (GE Healthcare Life Sciences, Freiburg, Germany).

Mass spectrometric analyses

Stably transfected HEK-mock or HEK-MT2-Myc-His cells grown in 25 cm^2-flasks were transiently transfected with 12 µg pEXPR-Strep-APP770$^{\Delta KPI}$ by lipofection with Lipofectamine^{TM} 2000 (Life Technologies) in the presence of Opti-MEM (Life Technologies) according to the manufacturer's instructions. After 24 hours, Aβ was immunoprecipitated from conditioned medium with 4G8 antibody (epitope 18-22; Covance) and magnetic beads conjugated with Protein G (New England Biolabs, Frankfurt am Main, Germany). Protein G magnetic beads were washed twice in phosphate-buffered saline (PBS) and twice with ammonium acetate. Aβ was eluted twice with 300 µL of 50% acetic acid and vacuum dried.

In an alternative experiment 1 µg synthetic Aβ(1-42) (H1368; Bachem) was incubated overnight at 37°C with 1 µg recombinant His-tagged matriptase-2 in a total volume of 10 µl. His-tagged matriptase-2 was purified as described previously (Figure S4A) (Jäckle *et al.*, 2015).

The samples were subsequently analyzed by the Mass Spectrometry Unit, Institute of Biochemistry and Molecular Biology, University of Bonn. For MALDI-TOF measurements peptide solutions were desalted on Zip-Tip C18 (Merck Chemicals GmbH, Darmstadt, Germany), eluates dried in a vacuum concentrator and redissolved in 4 µl TFA 0.1 %. 1 µl was mixed with 1 µl matrix solution (ACN 50 %, TFA 0.1 %) on a ground steel target and analyzed in reflectron mode MALDI-TOF (autoflex III, Bruker Daltonik GmbH, Bremen, Germany). Data were processed and visualized with FlexAnalysis Software (Bruker Daltonik).

For LC-MS analysis peptides were dissolved in 8 µl 0.1% trifluoroacetic acid. 1.5 µl were injected onto a C18 trap column (20 mm length, 100 µm inner diameter) coupled to a C18 analytical column (200 mm length, 75 µm inner diameter), made in house with 1.9 µm

ReproSil-Pur 120 C18-AQ particles (Dr. Maisch, Ammerbuch, Germany). Solvent A was 0.1% formic acid. Peptides were separated during a linear gradient from 4% to 40% solvent B (80% acetonitrile, 0.1% formic acid) within 80 min at a flow rate of 320 nl/min. The nanoHPLC was coupled online to an LTQ Orbitrap Velos mass spectrometer (Thermo Fisher Scientific, Bremen, Germany). Ions between 330 and 1600 m/z were scanned in the Orbitrap detector with a resolution of 30,000 (maximum fill time 400 ms, AGC target 10^6). The 25 most intense precursor ions (threshold intensity 5000) were subjected to collision induced dissociation and fragments analyzed in the linear ion trap. Fragmented peptide ions were excluded from repeat analysis for 15 s. Raw data processing and analysis of database searches were performed with Proteome Discoverer software 2.0.0.802 (Thermo Fisher Scientific). Peptide identification was done with an in house Mascot server version 2.5.1 (Matrix Science Ltd, London, UK). Data were searched against human sequences from SwissProt (release 2015_03). Precursor Ion m/z tolerance was 10 ppm, fragment ion tolerance 0.6 Da. Tryptic peptides were searched with up to two missed cleavages. Low scoring spectrum matches were searched again with semitryptic specificity with up to one missed cleavage. Oxidation (Met) and acetylation (protein N-terminus) were set as dynamic modifications. Mascot results from searches against SwissProt were sent to the percolator algorithm version 2.05 (Kall *et al.*, 2008) as implemented in Proteome Discoverer. Only proteins with two peptides (maximum posterior error probability 1%) were considered identified.

Statistical analysis

Statistical analysis was performed with standard statistical functions of GraphPad Prism using a two-tailed t test. If not stated otherwise, all values represent means ± SD. The error probability was set at $p<0.05$ (indicated in Figures by *), $p<0.01$ (**) or $p<0.001$ (***).

Acknowledgements

The authors thank Dr. Marc Sylvester (Mass Spectrometry Unit, Institute of Biochemistry and Molecular Biology, University of Bonn) for performing MS experiments.

A.M.B. and M.S. are supported by the German Research Foundation (DFG) Grant STI 660/1-1. M.M. and M.S. are supported by the Maria von Linden Program of the Gender Equality Center of the University of Bonn. J.W. is supported by the Collaborative Research Center SFB 645 “Regulation and manipulation of information flow within dynamic protein and lipid environments” funded by the DFG. C.B.-P. is supported by the SFB 877 “Proteolysis as a Regulatory Event in Pathophysiology” (project A9) and grant BE 4086/2-1 funded by the DFG.

References

Beckmann, A.-M., Maurer, E., Lülsdorff, V., Wilms, A., Furtmann, N., Bajorath, J., Gütschow, and Stirnberg, M., (2016). En route to new therapeutic options for iron overload diseases: Matriptase-2 as a target for Kunitz-type inhibitors. ChemCioChem, Epub ahead of print, DOI: 10.1002/cbic.201500651.

Bhasin, R., Van Nostrand, W.E., Saitoh, T., Donets, M.A., Barnes, E.A., Quitschke, W.W., and Goldgaber, D. (1991). Expression of active secreted forms of human amyloid beta-protein precursor by recombinant baculovirus-infected insect cells. Proc. Natl. Acad. Sci. USA *88*, 10307-10311.

Bugge, T.H., List, K., and Szabo, R. (2007). Matriptase-dependent cell surface proteolysis in epithelial development and pathogenesis. Front. Biosci. *12*, 5060-5070.

Dosa, S., Stirnberg, M., Lülsdorff, V., Häussler, D., Maurer, E., and Gütschow, M. (2012). Active site mapping of trypsin, thrombin and matriptase-2 by sulfamoyl benzamidines. Bioorg. Med. Chem. *20*, 6489-6505.

Du, X., She, E., Gelbart, T., Truksa, J., Lee, P., Xia, Y., Khovananth, K., Mudd, S., Mann, N., Moresco, E.M., Beutler, E., and Beutler, B. (2008). The serine protease TMPRSS6 is required to sense iron deficiency. Science *320*, 1088-1092.

Eigenbrot, C., Ganesan, R., and Kirchhofer, D. (2010). Hepatocyte growth factor activator (HGFA): molecular structure and interactions with HGFA inhibitor-1 (HAI-1). FEBS J. *277*, 2215-2222.

Evan, G.I., Lewis, G.K., Ramsay, G., and Bishop, J.M. (1985). Isolation of monoclonal antibodies specific for human c-myc proto-oncogene product. Mol. Cell. Biol. *5*, 3610-3616.

Farady, C.J. and Craik, C.S. (2010). Mechanisms of macromolecular protease inhibitors. ChemBioChem *11*, 2341-2346.

Finberg, K.E., Whittlesey, R.L., Fleming, M.D., and Andrews, N.C. (2010). Down-regulation of Bmp/Smad signaling by Tmprss6 is required for maintenance of systemic iron homeostasis. Blood *115*, 3817-3826.

Finberg, K.E., Heeney, M.M., Campagna, D.R., Aydinok, Y., Pearson, H.A., Hartman, K.R., Mayo, M.M., Samuel, S.M., Strouse, J.J., Markianos, K., *et al.* (2008). Mutations in TMPRSS6 cause iron-refractory iron deficiency anemia (IRIDA). Nat. Genet. *40*, 569-571.

Folgueras, A.R., de Lara, F.M., Pendas, A.M., Garabaya, C., Rodriguez, F., Astudillo, A., Bernal, T., Cabanillas, R., Lopez-Otin, C., and Velasco, G. (2008). Membrane-bound serine protease matriptase-2 (Tmprss6) is an essential regulator of iron homeostasis. Blood *112*, 2539-2545.

Goldgaber, D., Lerman, M.I., McBride, O.W., Saffiotti, U., and Gajdusek, D.C. (1987). Characterization and chromosomal localization of a cDNA encoding brain amyloid of Alzheimer's disease. Science *235*, 877-880.

Graham, F.L., Smiley, J., Russell, W.C., and Nairn, R. (1977). Characteristics of a human cell line transformed by DNA from human adenovirus type 5. J. Gen. Virol. *36*, 59-74.

Hooper, J.D., Clements, J.A., Quigley, J.P., and Antalis, T.M. (2001). Type II transmembrane serine proteases. Insights into an emerging class of cell surface proteolytic enzymes. J. Biol. Chem. *276*, 857-860.

Jäckle, F., Schmidt, F., Wichert, R., Arnold, P., Prox, J., Mangold, M., Ohler, A., Pietrzik, C.U., Koudelka, T., Tholey, A., *et al.* (2015). Metalloprotease meprin beta is activated by transmembrane serine protease matriptase-2 at the cell surface thereby enhancing APP shedding. Biochem. J. *470*, 91-103.

Jiang, J., Yang, J., Feng, P., Zuo, B., Dong, N., Wu, Q., He, Y. (2014). N-glycosylation is required for matriptase-2 autoactivation and ectodomain shedding. J. Biol. Chem. *289*, 19500-19507.

Kall, L., Storey, J.D., MacCoss, M.J., and Noble, W.S. (2008). Assigning significance to peptides identified by tandem mass spectrometry using decoy databases. J. Proteome Res. *7*, 29-34.

Krijt, J., Fujikura, Y., Ramsay, A.J., Velasco, G., and Necas, E. (2011). Liver hemojuvelin protein levels in mice deficient in matriptase-2 (Tmprss6). Blood Cells Mol. Dis. *47*, 133-137.

LaFerla, F.M. and Oddo, S. (2005). Alzheimer's disease: Aβ, tau and synaptic dysfunction. Trends Mol. Med. *11*, 170-176.

Lin, C.Y., Anders, J., Johnson, M., and Dickson, R.B. (1999). Purification and characterization of a complex containing matriptase and a Kunitz-type serine protease inhibitor from human milk. J. Biol. Chem. *274*, 18237-18242.

Lin, C.Y., Tseng, I.C., Chou, F.P., Su, S.F., Chen, Y.W., Johnson, M.D., and Dickson, R.B. (2008). Zymogen activation, inhibition, and ectodomain shedding of matriptase. Front. Biosci. *13*, 621-635.

Maurer, E., Gütschow, M., and Stirnberg, M. (2013). Hepatocyte growth factor activator inhibitor type 2 (HAI-2) modulates hepcidin expression by inhibiting the cell surface protease matriptase-2. Biochem. J. *450*, 583-593.

Maurer, E., Sisay, M.T., Stirnberg, M., Steinmetzer, T., Bajorath, J., and Gütschow, M. (2012). Insights into matriptase-2 substrate binding and inhibition mechanisms by analyzing active-site-mutated variants. ChemMedChem *7*, 68-72.

Maxson, J,E., Chen, J., Enns, C.A., and Zhang, A.S. (2010). Matriptase-2- and proprotein convertase-cleaved forms of hemojuvelin have different roles in the down-regulation of hepcidin expression. J. Biol. Chem. *285*, 39021-39028.

Miller, G.S. and List, K. (2013). The matriptase-prostasin proteolytic cascade in epithelial development and pathology. Cell. Tissue Res. *351*, 245-253.

Rogers J.T., Randall, J.D., Cahill, C.M., Eder, P.S., Huang, X., Gunshin, H., Leiter, L., McPhee, J., Sarang, S.S., Utsuki, T., *et al.* (2002). An iron-responsive element type II in the *5*'-untranslated region of the Alzheimer's amyloid precursor protein transcript. J. Biol. Chem. *277*, 45518-45528.

Sastre, M., Steiner, H., Fuchs, K., Capell, A., Multhaup, G., Condron, M.M., Teplow, D.B., and Haass, C. (2001). Presenilin-dependent gamma-secretase processing of beta-amyloid precursor protein at a site corresponding to the S3 cleavage of Notch. EMBO Rep. *2*, 835-841.

Schmaier, A.H., Dahl, L.D., Hasan, A.A., Cines, D.B., Bauer, K.A., and Van Nostrand, W.E. (1995). Factor IXa inhibition by protease nexin-2/amyloid beta-protein precursor on phospholipid vesicles and cell membranes. Biochemistry *34*, 1171-1178.

Selkoe, D.J. (1991). The molecular pathology of Alzheimer's disease. Neuron *6*, 487-498.

Shimokawa, M., Nakamura, K., Maruyama, K., Tagawa, K., Miyatake, T., Sugita, H., Ishiura, S., and Suzuki, K. (1993). Inhibitory spectra of purified protease nexin-II and related proteins towards cellular proteinases. Biochimie *75*, 911-915.

Silvestri, L., Pagani, A., Nai, A., De Domenico, I., Kaplan, J., and Camaschella, C. (2008). The serine protease matriptase-2 (TMPRSS6) inhibits hepcidin activation by cleaving membrane hemojuvelin. Cell. Metab. *8*, 502-511.

Sisay, M.T., Steinmetzer, T., Stirnberg, M., Maurer, E., Hammami, M., Bajorath, J., and Gütschow, M. (2010). Identification of the first low-molecular-weight inhibitors of matriptase-2. J. Med. Chem. *53*, 5523-5535.

Sisodia, S.S. (1992). Beta-amyloid precursor protein cleavage by a membrane-bound protease. Proc. Natl. Acad. Sci. USA *89*, 6075-6079.

Stirnberg, M., Maurer, E., Horstmeyer, A., Kolp, S., Frank, S., Bald, T., Arenz, K., Janzer, A., Prager, K., Wunderlich, P., *et al.* (2010). Proteolytic processing of the serine protease matriptase-2: identification of the cleavage sites required for its autocatalytic release from the cell surface. Biochem. J. *430*: 87-95.

Van Nostrand, W.E., Wagner, S.L., Farrow, J.S., and Cunningham, D.D. (1990). Immunopurification and protease inhibitory properties of protease nexin-2/amyloid beta-protein precursor. J. Biol. Chem. *265*, 9591-9594.

Van Nostrand, W.E., Wagner, S.L., Suzuki, M., Choi, B.H., Farrow, J.S., Geddes, J.W., Cotman, C.W., and Cunningham, D.D. (1989). Protease nexin-II, a potent antichymotrypsin, shows identity to amyloid beta-protein precursor. Nature *341*, 546-549.

Vassar, R, Bennett, B.D., Babu-Khan, S., Kahn, S., Mendiaz, E.A., Denis, P., Teplow, D.B., Ross, S., Amarante, P., Loeloff, R., *et al.* (1999). Beta-secretase cleavage of Alzheimer's amyloid precursor protein by the transmembrane aspartic protease BACE. Science *286*, 735-741.

Velasco, G., Cal, S., Quesada, V., Sanchez, L.M., and Lopez-Otin, C. (2002). Matriptase-2, a membrane-bound mosaic serine proteinase predominantly expressed in human liver and showing degrading activity against extracellular matrix proteins. J. Biol. Chem. *277*, 37637-37646.

Wong, B,X., Tsatsanis, A., Lim, L.Q., Adlard, P.A., Bush, A.I., and Duce, J.A. (2014). beta-Amyloid precursor protein does not possess ferroxidase activity but does stabilize the cell surface ferrous iron exporter ferroportin. PLoS One *9*, e114174.

Zheng, H., and Koo, E.H. (2011). Biology and pathophysiology of the amyloid precursor protein. Mol. Neurodegener. *6*, 27.

Tables and figures

Table 1 Identified Aβ peptides by LC-MS analysis of samples shown in Figure S4.

Position in Aβ	Aβ	Aβ + MT2
1-16	[M].DAEFRHDSGYEVHHQK.[L]	[M].DAEFRHDSGYEVHHQK.[L]
4-16		[E].FRHDSGYEVHHQK.[L]
6-17		[R].HDSGYEVHHQKL.[V]
6-28		[R].HDSGYEVHHQKLVFFAEDVGSNK.[G]
16-28	[Q].KLVFFAEDVGSNK.[G]	[Q].KLVFFAEDVGSNK.[G]
17-28		[K].LVFFAEDVGSNK.[G]
17-29		[K].LVFFAEDVGSNKG.[A]
18-28		[L].VFFAEDVGSNK.[G]

The single-letter amino acid code is used.

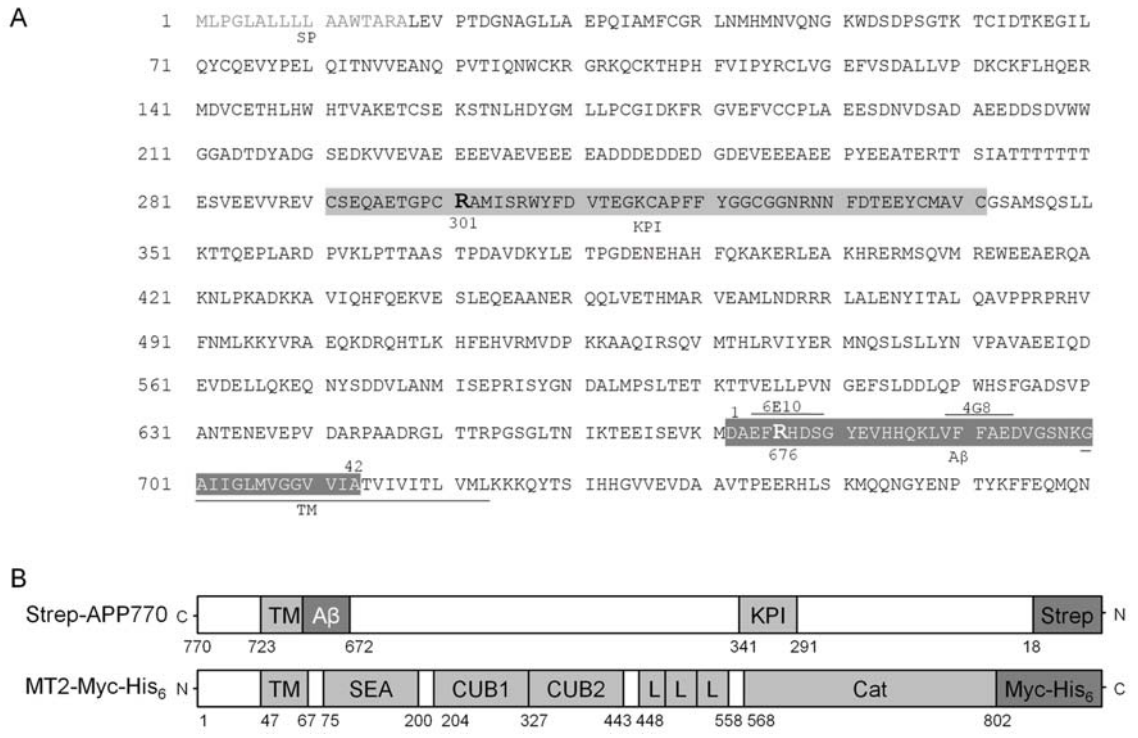

Figure 1 Schematic illustration of the amino acid sequence and domain organization of human APP770.

(A) The amino acid numbering of APP770 starts from the N-terminus with the signal peptide (SP) shown in light black. The Kunitz protease inhibitor domain (KPI) is highlighted in grey, the Aβ region numbered from 1-42 is highlighted in black and the transmembrane (TM) domain is underlined. The epitopes recognized by antibodies 4G8 and 6E10 are indicated.

Amino acids mutated in this study are given in bold type (Arg^{301}, Arg^{676}). (B) The type I transmembrane protein APP770 was cloned as a fusion construct with an N-terminal Strep-tag (Strep-APP770), the type II transmembrane protein matriptase-2 was cloned as a fusion construct with a C-terminal Myc- and His-tag (MT2-Myc-His). After expression, all tags are exposed at the cell surface. Cat, serine protease catalytic domain; CUB, complement factor C1s/1r, urchin embryonic growth factor, BMP domain; L, low-density lipoprotein receptor class A domain; SEA, sea urchin sperm protein, enteropeptidase, agrin domain; TM, transmembrane domain.

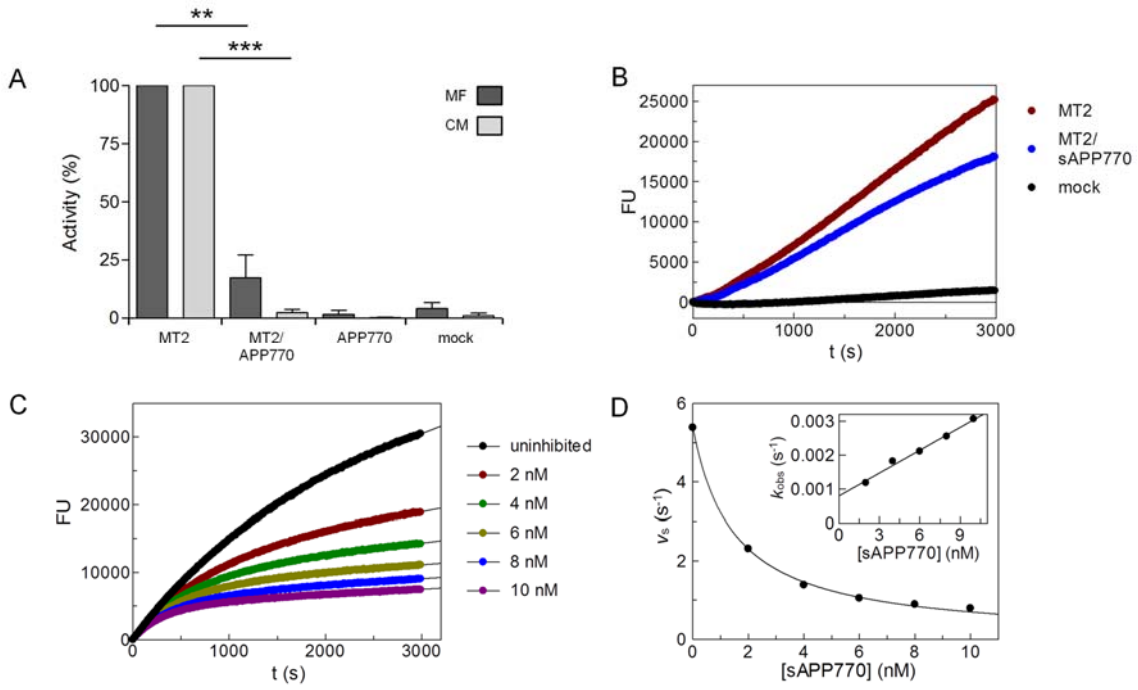

Figure 2 Inhibition of matriptase-2 proteolytic activity by APP770.

(A) HEK-mock and HEK-MT2-Myc-His cells either alone or transiently transfected with pEXPR-Strep-APP770 were cultured for 2 days with Opti-MEM. Total protein from membrane fractions (20 µg; MF) or concentrated conditioned media (5 µg; CM) was incubated with 200 µM Boc-QAR-*para*-nitroanilide as a substrate. The release of *para*-nitroaniline was monitored at a wavelength of 405 nm for 20 min at 37°C. The resulting activities were normalized to proteolytic activity in concentrated media derived from HEK-MT2-Myc-His cells and measured in duplicate in at least two independent experiments. (B) Matriptase-2 activity was measured at the surface of intact HEK-MT2-Myc-His cells or HEK-mock cells grown on a 96-well plate. The reaction was started by adding 40 µM of the fluorogenic substrate Boc-QAR-AMC and 30 nM of purified sAPP770 and subsequently

followed at 37°C for 50 min. Data points for HEK-mock and HEK-MT2-Myc-His cells were shown previously (Beckmann *et al.*, 2016). (C) Different amounts of purified sAPP770 were incubated with conditioned media derived from matriptase-2-expressing HEK cells in the presence of 40 µM of the fluorogenic substrate Boc-QAR-AMC. The release of 7-amino-4-methylcoumarin from the fluorogenic substrate was monitored with an excitation wavelength of 340 nm and emission wavelength of 460 nm over 50 min at 37°C. (D) The progress curves were analyzed by nonlinear regression using the slow-binding equation. The final steady-state rates v_s were plotted versus inhibitor concentrations to obtain an IC_{50} value which corresponds to $K_i\,(1 + [S]/K_m)$. Inset; The replot of k_{obs} values versus inhibitor concentrations is linear and the on (k_{on} = 5.0×10^{-4} s^{-1} nM^{-1}) and off (k_{off} = 8.0×10^{-4} s^{-1}) rate constants for inhibitor association/dissociation were obtained.

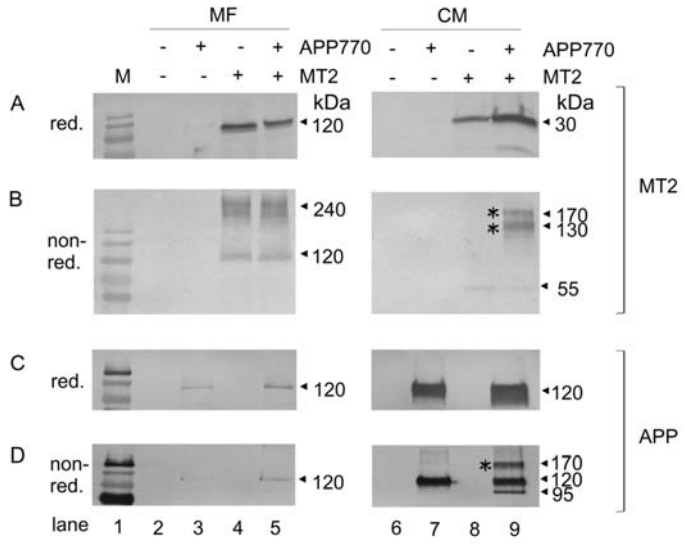

Figure 3 Stable complex formation of matriptase-2 and APP770.

HEK-mock and HEK-MT2-Myc-His cells were left untreated or transiently transfected with pEXPR-Strep-APP770 and cultured for 2 days with Opti-MEM. Total protein (30 µg) of membrane fractions (left panels) or conditioned media (right panels) were separated under reducing conditions (A, C) or non-reducing conditions (B, D) prior immunoblotting. Matriptase-2 was detected using the monoclonal mouse anti-c-Myc antibody (A, B), APP was detected using the Strep-Tactin AP conjugate (C, D). Representative immunoblots from three independent experiments are shown. M, molecular mass markers; non-red., non-reducing; red., reducing. Formation of APP770/matriptase-2-complexes at 130 kDa and 170 kDa were marked with asterisks.

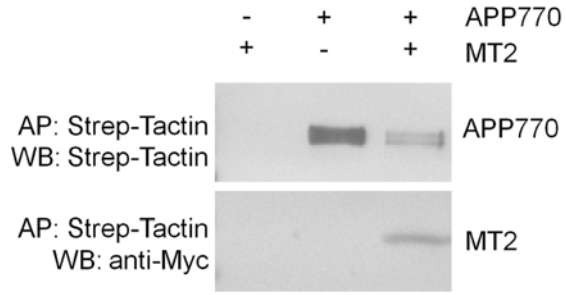

Figure 4 Co-purification of matriptase-2 and APP770 by affinity chromatography. Conditioned media (400 µg total protein) of HEK-MT2-Myc-His or HEK-mock cells either untreated or transiently transfected with pEXPR-Strep-APP770, were subjected to affinity chromatography using the Strep-tag purification technique. Elution fractions were analyzed by western blotting using either the anti-c-Myc antibody or the Strep-Tactin alkaline phosphatase conjugate. AP, affinity purification.

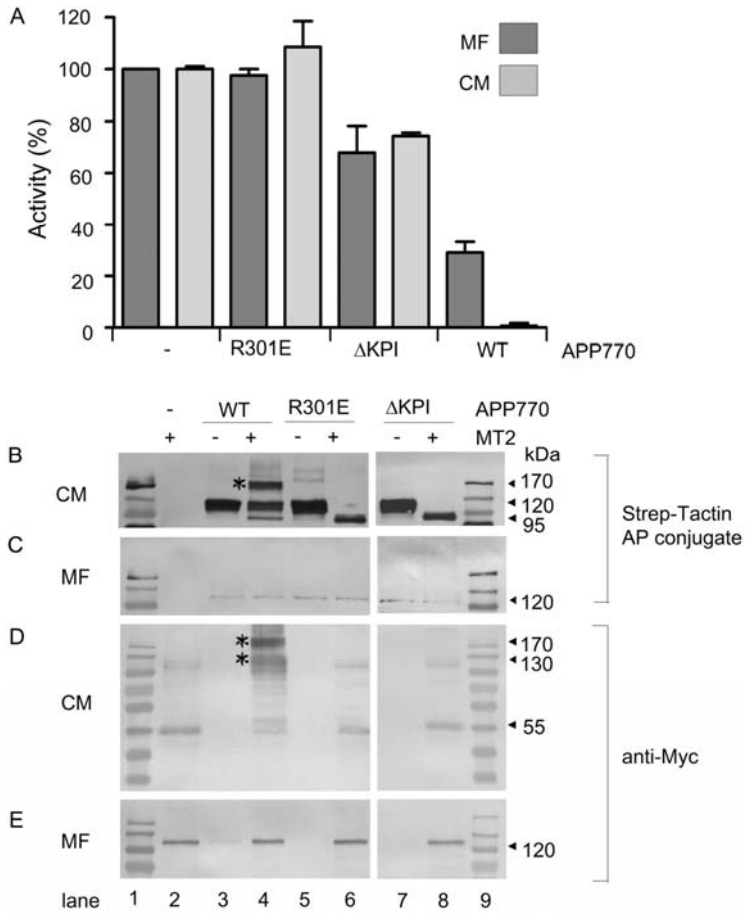

Figure 5 Influence of KPI on the inhibitory potential of APP770 and formation of matriptase-2/APP770 complexes.

HEK-MT2-Myc-His cells either alone or transiently transfected with pEXPR-Strep-APP770, pEXPR-Strep-APP770^{R301E} or pEXPR-Strep-APP770$^{\Delta KPI}$ were cultured for 2 days with Opti-MEM. (A) Total protein from membrane fractions (20 µg; MF) or concentrated conditioned media (5 µg; CM) was incubated with 200 µM Boc-QAR-*para*-nitroanilide as a substrate. The release of *para*-nitroaniline was monitored at a wavelength of 405 nm for 20 min at 37°C. The resulting activities were normalized to proteolytic activity in concentrated media derived from HEK-MT2-Myc-His cells and measured in duplicate in at least two independent experiments. (B)-(E) Total protein from conditioned media (30 µg; CM; B, D) was separated under non-reducing conditions, total protein from membrane fractions (30 µg; MF; C, E) was separated under reducing conditions prior to electroblotting and detection of APP with Strep-Tactin AP conjugate (B, C) and matriptase-2 with the anti-c-Myc antibody as shown in (D, E). Lanes 1 and 9, molecular mass markers. Formation of APP770/matriptase-2-complexes at 130 kDa and 170 kDa were marked with asterisks.

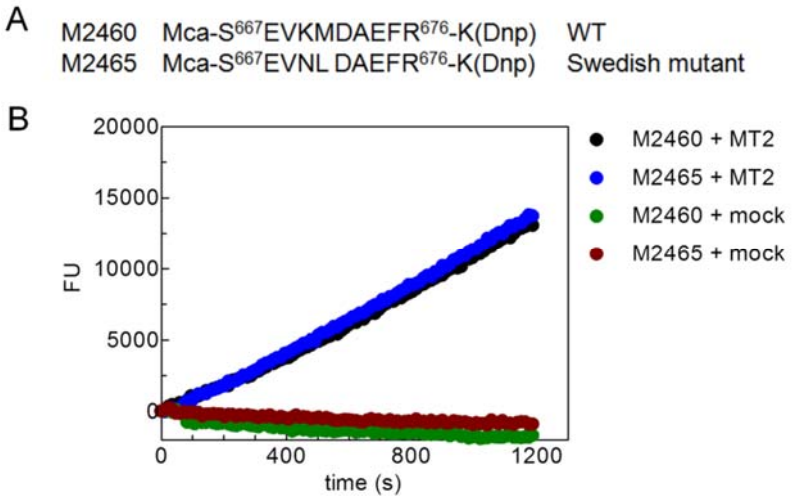

Figure 6 Cleavage of APP peptides.

(A) Equal amounts of proteins from conditioned media of HEK-mock or HEK-MT2-Myc-His cells were incubated with 40 µM of the quenched fluorogenic peptide substrates M2460 or M2465 for 20 min at 37°C. In these fluorescence-quenching substrates, the fluorescence of 7-amino-4-methylcoumarin is quenched by Dnp (2,4-Dinitrophenyl). Upon cleavage, the fluorescence was recovered and monitored with an excitation wavelength of 340 nm and emission wavelength of 460 nm. (B) The amino acid sequence of M2460 represents the β-secretase cleavage site of wild type APP, the sequence of M2465 represents the β-secretase cleavage site of the Swedish mutant of APP.

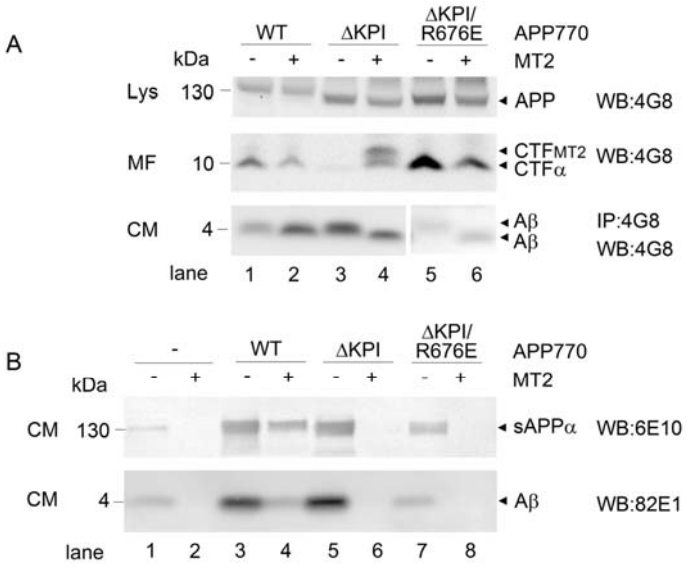

Figure 7 Generation of truncated Aβ by matriptase-2.

HEK-mock or HEK-MT2-Myc-His cells were left untreated or transfected with wild type APP770, APP770$^{\Delta KPI}$ or APP770$^{\Delta KPI/R676E}$ and cultured for 2 days with Opti-MEM. (A) After immunoprecipitation with antibody 4G8 (epitope within amino acids 18-22 of Aβ or 689-693 of APP), secretion of Aβ was analyzed in conditioned media (CM). Total protein (30 µg) of lysates (Lys) and membrane fractions (MF) were analyzed as controls visualizing full length APP in lysates and C-terminal fragments (CTF) in membrane fractions using the same antibody. (B) Total protein (30 µg) of conditioned media (CM) was analyzed with antibodies 6E10 (epitope within amino acids 3-8 of Aβ or 674-679 of APP) and 82E1 (neoepitope within amino acids 1-5 of Aβ) visualizing sAPPα and Aβ.

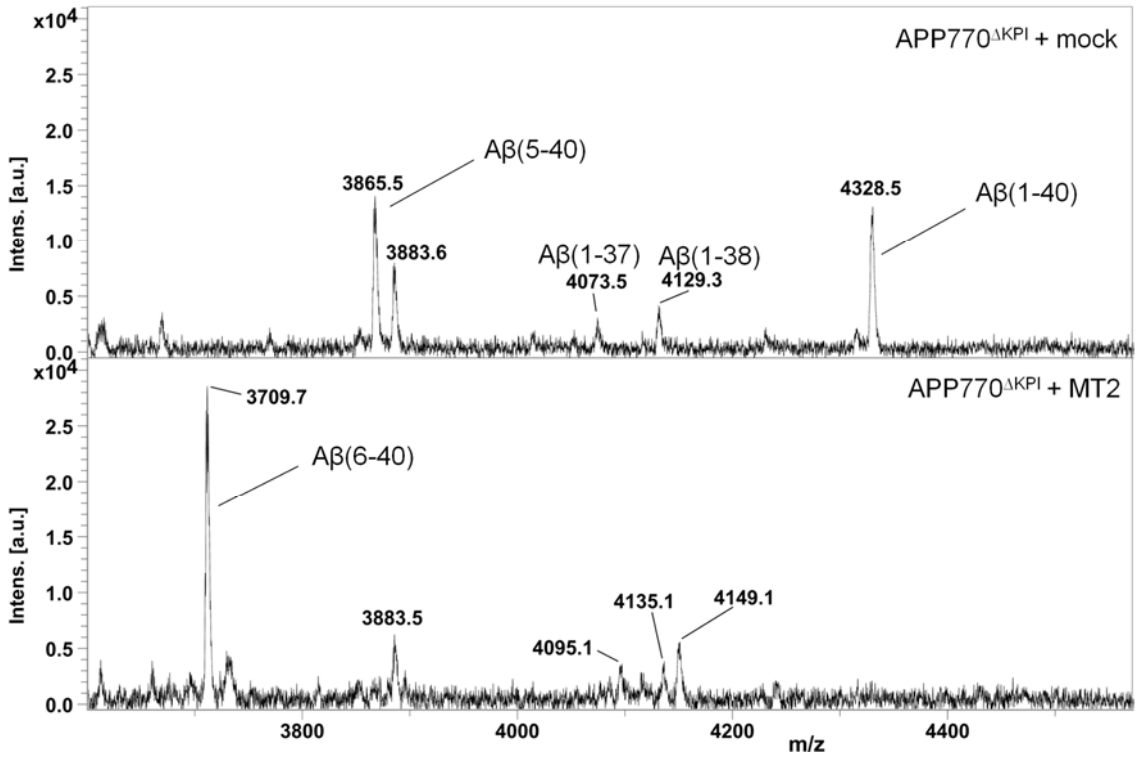

Figure 8 Proteomic identification of Aβ generated in HEK cells expressing APP770$^{\Delta KPI}$ and matriptase-2.

Stably transfected HEK-mock or HEK-MT2-Myc-His cells were transiently transfected with pEXPR-Strep-APP770$^{\Delta KPI}$. Aβ was immunoprecipitated from conditioned media with 4G8 antibody (epitope 18-22) prior MALDI-TOF analyses. Upper spectrum: Aβ immunoprecipitated after expression of APP770$^{\Delta KPI}$ in HEK-mock cells; lower spectrum: Aβ immunoprecipitated after expression of APP770$^{\Delta KPI}$ in HEK-MT2-Myc-His cells. Range 3600-4600 m/z. Peak detection of average m/z. Theoretical and observed masses for Aβ(1-40) are 4328.2/4328.5 m/z, for Aβ(6-40) 3709.9/3709.7 m/z, for Aβ(5-40) 3866.0/3865.5 m/z, for Aβ(1-37) 4073.0/4073.5 m/z and for Aβ(1-38) 4130.0/4129.3 m/z, respectively.

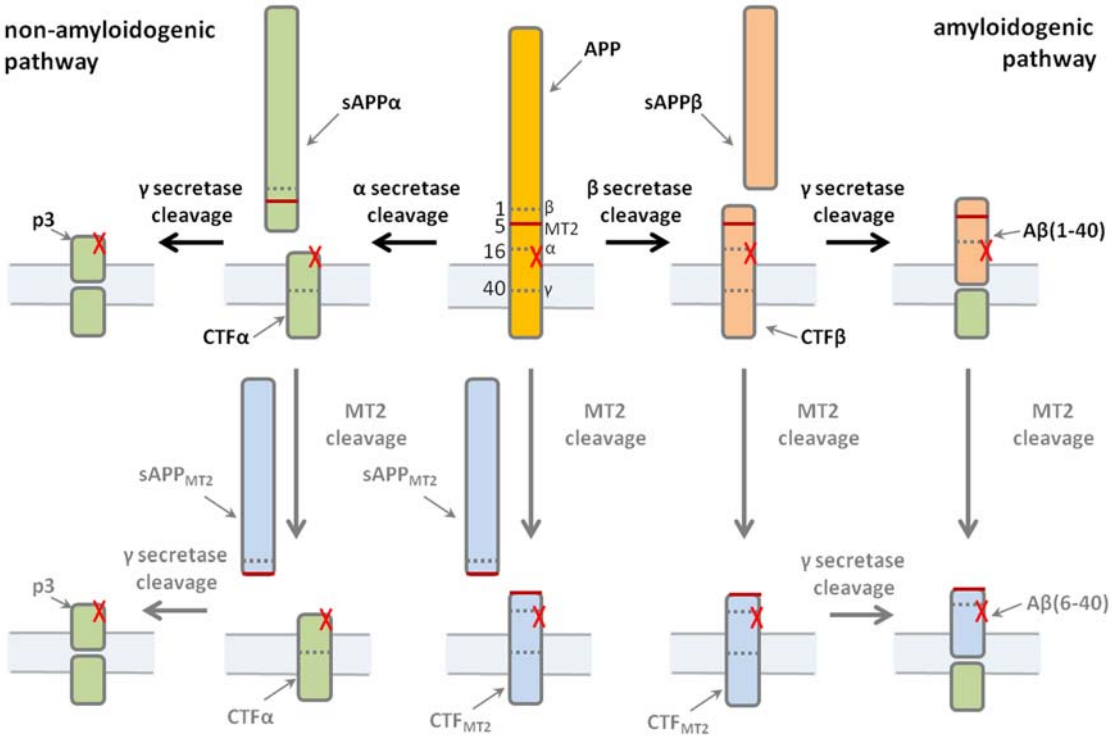

Figure 9 Processing of APP.

APP can be processed either by α- or β-secretase producing extracellular soluble N-terminal fragments (sAPPα or sAPPβ) and membrane-bound C-terminal fragments (CTFα or CTFβ). Without the KPI domain APP can be additionally processed by matriptase-2 producing $sAPP_{MT2}$ and CFT_{MT2}. CTFs can be further degraded by the action of γ-secretase generating the small p3 fragment, Aβ(1-40) or Aβ(6-40). The recognition site for antibody 4G8 is indicated by a red cross mark. Cleavage sites for α-, β- and γ-secretases are indicated by a grey dash line, the cleavage site for matriptase-2 is indicated by a red line. All cleavage sites within full length APP are also indicated by amino acid numbers (numbering corresponds to Aβ peptide).

Supplementary figures

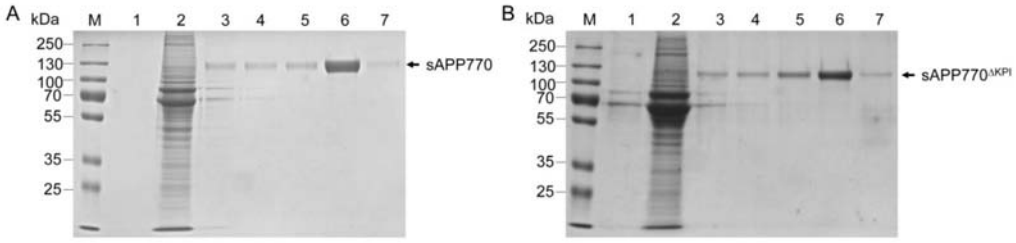

Figure S1. Purification of recombinant sAPP770 and sAPP770ΔKPI.

HEK cells transiently transfected with pEXPR-Strep-APP770 or pEXPR-Strep-APP770ΔKPI were cultured for 2 days with Opti-MEM. Conditioned medium was concentrated and subjected to Strep-Tactin affinity chromatography to isolate the soluble form of APP770 or APP770ΔKPI. Purity of isolated sAPP770 (A) and sAPP770ΔKPI (B) was confirmed by SDS-PAGE followed by Coomassie Brilliant Blue staining. Lane 1, flow-through; lane 2, wash fraction 1; lane 3, wash fraction 5; lanes 4-7, elution fractions; M, molecular mass markers.

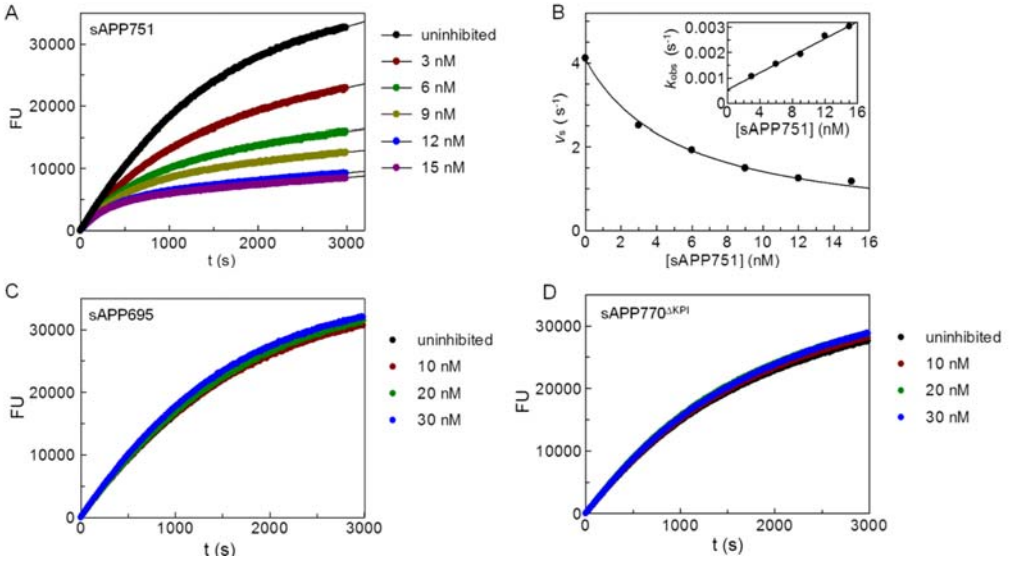

Figure S2. Inhibition of matriptase-2 by sAPP751, sAPP695 and sAPP770ΔKPI.

The activity of matriptase-2 in concentrated media of stably transfected HEK-MT2-Myc-His cells in the presence of different concentrations of purified sAPP751 (A) and (B), sAPP695

(C) or sAPP770ΔKPI (D) was measured by monitoring the cleavage of the fluorogenic substrate Boc-QAR-AMC. Soluble APP751 and APP695 were purified as described previously (Jefferson, T., Causevic, M., auf dem Keller, U., Schilling, O., Isbert, S., Geyer, R., Maier, W., Tschickardt, S., Jumpertz, T., Weggen, S., Bond, J. S., Overall, C. M., Pietrzik, C. U., and Becker-Pauly, C. (2011) Metalloprotease meprin beta generates nontoxic N-terminal amyloid precursor protein fragments in vivo. J. Biol. Chem. 286, 27741-27750). (A) Different amounts of purified sAPP751 were incubated with conditioned media derived from matriptase-2-expressing HEK cells and the reaction was followed over 50 min at 37°C. (B) The progress curves were analyzed by nonlinear regression using the slow-binding equation. The final steady-state rates *v*s were plotted versus inhibitor concentrations to obtain an IC50 value which corresponds to *K*i (1 + [S]/*K*m) of 2.1 ± 0.1 nM. Inset; The replot of *k*obs values versus inhibitor concentrations is linear and the on (*k*on = 4.5×10-4 s-1 nM-1) and off (*k*off = 4.7×10-4 s-1) rate constants for inhibitor association/dissociation were obtained. (C, D) Different amounts of purified sAPP695 (C) or sAPP770ΔKPI (D) were incubated with conditioned media derived from matriptase-2-expressing HEK cells and the reaction was followed over 50 min at 37°C.

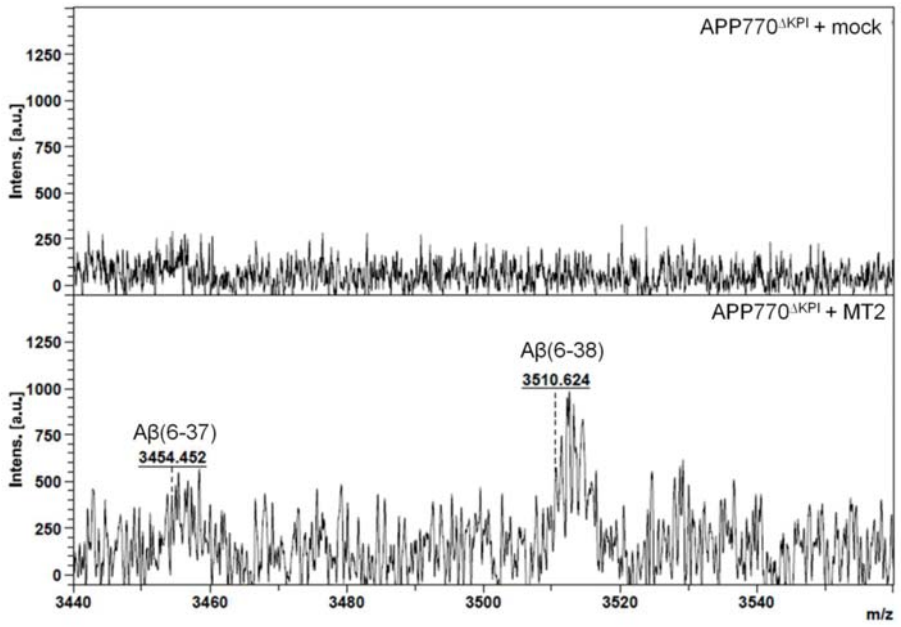

Figure S3. Proteomic identification of Aβ generated in HEK cells expressing APP770ΔKPI and matriptase-2.

Stably transfected HEK-mock or HEK-MT2-Myc-His cells were transiently transfected with pEXPR-Strep-APP770ΔKPI. Aβ was immunoprecipitated from conditioned media with 4G8 antibody (epitope 18-22) prior MALDI-TOF analyses. Upper spectrum: Aβ immunoprecipitated after expression of APP770ΔKPI in HEK-mock cells; lower spectrum: Aβ immunoprecipitated after expression of APP770ΔKPI in HEK-MT2-Myc-His cells. Range 3440-3560 m/z. Peak detection of average m/z. Theoretical and observed masses for Aβ(6-37) and Aβ(6-38) are 3454.7/3454.5 m/z and 3511.7/3510.6 m/z, respectively.

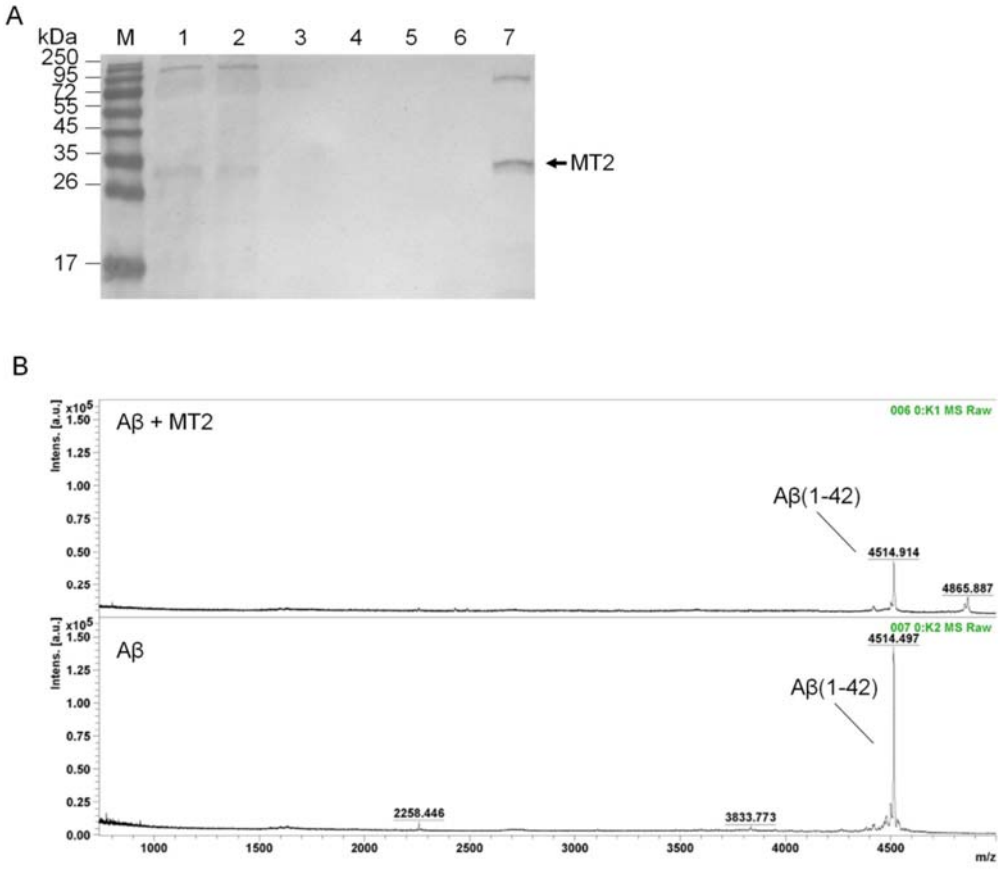

Figure S4. Mass spectrometric analysis of synthetic Aβ.

(A) Matriptase-2 was purified from the concentrated conditioned medium of stably transfected HEK-MT2-Myc-His cells by affinity chromatography using 250 mM imidazole and subsequently analyzed by western blotting using c-Myc antibody. (B) An amount of 1 µg synthetic Aβ(1-42) (H1368; Bachem) was incubated overnight at 37°C with ca. 1 µg recombinant His-tagged matriptase-2 in a total volume of 10 µl. The samples (upper spectrum: Aβ incubated with matriptase-2; lower spectrum: Aβ alone) were analyzed by MALDI-TOF by the Mass Spectrometry Unit, Institute of Biochemistry and Molecular Biology, University of Bonn. Range 740-5000 m/z. Peak detection of average m/z.